Available online at www.sciencedirect.com
SCIENCE DIRECT®
ELSEVIER
Optics Communications 228 (2003) 155–160
OPTICS COMMUNICATIONS
www.elsevier.com/locate/optcom

Orbital angular momentum of photons in noncollinear parametric downconversion

Gabriel Molina-Terriza *,1, Juan P. Torres, Lluis Torner

ICFO—Institut de Ciencies Fotoniques and Department of Signal Theory and Communications, Universitat Politecnica de Catalunya, 08034 Barcelona, Spain

Received 6 June 2003; received in revised form 24 September 2003; accepted 24 September 2003

Abstract

Conservation of the orbital angular momentum (OAM) of light in photon downconversion has been observed experimentally in nearly collinear phase-matching geometries, where the pump, signal and idler photons propagate along almost the same direction [Nature 412 (2001) 313]. However, here we predict that such paraxial measurements conducted with entangled photons in noncollinear geometries are not expected to comply with OAM conservation in the above sense. Under proper conditions, the strength of such apparent anomaly approaches 100%. We discuss the physical origin of the effect and suggest experimental schemes where it can be verified.

PACS: 03.67.−a; 42.50.−p; 42.25.−p

Keywords: Orbital angular momentum; Spontaneous parametric downconversion

1. Introduction

The angular momentum of light plays an emerging role in both classical and quantum science, with important applications in areas as diverse as biophotonics, micromachines, spintronics, or quantum information. The angular momentum of light contains a spin contribution, dictated by the polarization of the electromagnetic fields [1], and an orbital contribution, related to their spatial structure [2]. In general, only the total angular momentum is an observable quantity [3]. However, within the paraxial regime, both contributions can be measured and manipulated separately [4–6]. While the spin angular momentum is extensively employed in quantum information schemes, only recently the orbital angular momentum (OAM) has been added to the toolkit. In particular, a recent landmark experiment demonstrated that the idler and signal photons produced in the process of spontaneous parametric downconversion constitute an entangled state of OAM [7]. Therefore, because the OAM defines an infinite-dimensional

* Corresponding author. Tel.: +43-1-4277-51226; fax: +43-1-4277-9512.
E-mail address: gamote@quantum.at (G. Molina-Terriza).
1 Present address: Institut für Experimentalphysik, Universität Wien, Boltzmanngasse 5, A-1090 Vienna, Austria.

0030-4018/$ - see front matter
doi:10.1016/j.optcom.2003.09.071

Hilbert space, it can be employed to generate engineered multidimensional entangled states [8–10], hence, e.g., violation of Bell inequalities with qutrits encoded in OAM has been observed experimentally recently [11]. In parallel to the exploration of such possibilities, a fundamental question that arises is whether the OAM is conserved in the process of photon downconversion [12–14].

In collinear downconversion, the two-photon entangled state constituted by the signal and idler photons is described by a transverse mode function that is *globally paraxial*. Therefore, the OAM of all the involved photons is a well-defined quantity that in the absence of momentum transfer between light and matter must be conserved, a feature that within the experimental accuracy is consistent with the observations by Mair et al., in the quasi-collinear geometry used [7]. The question is how the conservation rule associated to such measurements extends to arbitrary noncollinear geometries. In such geometries, because of the conditions imposed by linear momentum conservation of photons, the generated two-photon entangled state can be also described by a mode function which is *locally paraxial* in a suitable transverse frame centered on the signal and idler wave vectors (see Fig. 1). Therefore, the paraxial OAM carried by each of the photons is also a well-defined quantity, which can be measured experimentally. However, the *global mode function* is not necessarily paraxial. On the contrary, in experimentally feasible downconversion processes in existing crystals it might depart largely from paraxiality in the global sense. Here we predict that well-defined, locally paraxial measurements of the OAM conducted with entangled photons generated in such noncollinear geometries yield anomalous outcomes, in the sense that they do not comply with paraxial angular momentum conservation. We show that, under proper conditions, the probability to detect anomalous values approaches ≈ 1.

Consider a downconversion process pumped by a continuous-wave photon source in a general

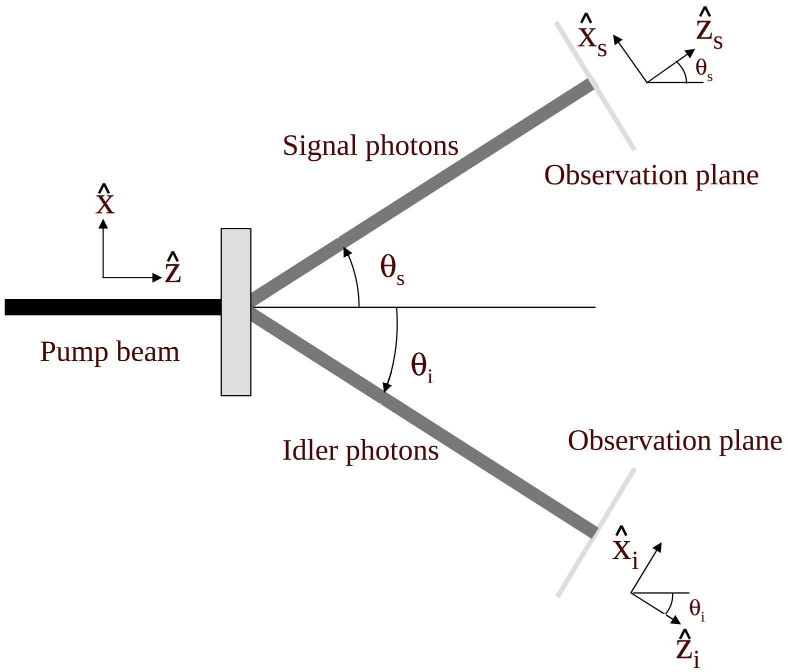

Fig. 1. Sketch of the noncollinear downconversion geometry, showing the propagation directions of the pump, signal, and idler photons.

noncollinear phase-matching geometry (Fig. 1). The two-photon quantum state $|\Psi\rangle$ at the output of the nonlinear crystal within the first order perturbation theory is given by $|\Psi\rangle = |0,0\rangle - \mathrm{i}/\hbar \int_0^\tau \mathrm{d}t H_\mathrm{I}(t)|0,0\rangle$, where $|0,0\rangle$ is the vacuum state, τ is the interaction time, and $H_\mathrm{I}(t)$ is the effective Hamiltonian in the interaction picture, given by [15–17]

$$H_\mathrm{I} = \epsilon_0 \int_V \mathrm{d}^3 V \chi^{(2)} \vdots E_p^+ E_s^- E_i^- + \mathrm{c.c}, \tag{1}$$

where ϵ_0 is the permittivity of free space, $\chi^{(2)}$ is the second order nonlinear susceptibility tensor, V is the volume of the crystal illuminated by the pump beam, E_p^+ refers to the positive-frequency part of the pump electric field operator and $E_{s,i}^-$ refers to the negative-frequency part of the signal and idler electric field operators. The paraxial pump beam is treated classically and written as

$$E_p(x,y,z,t) = \hat{e}_p \int \mathrm{d}\mathbf{q} \hat{\Phi}(\mathbf{q}) \times \exp[\mathrm{i}k_p(\mathbf{q})z + \mathrm{i}\mathbf{q}\cdot\mathbf{x} - \mathrm{i}\omega_p t] + \mathrm{c.c},$$

where ω_p is the angular frequency of the pump beam, $k_p(\mathbf{q}) = \sqrt{(\omega_p n_p/c)^2 - |\mathbf{q}|^2}$ is the longitudinal wave number inside the crystal, $\mathbf{q}$ is the transverse spatial frequency, n_p is the refractive index at the pump wavelength and $\hat{\Phi}(\mathbf{q})$ is the field profile of the pump beam in the spatial frequency domain at the input face of the crystal, and $\hat{e}_p$ is the polarization vector.

Because of the phase-matching conditions imposed by the nonlinear crystal, the wave vectors of the signal and idler mode functions belong to a narrow bundle around the central wave vectors, and can thus be written as $\vec{k}_s = \vec{k}_s^0 + \Delta\vec{k}_s$ and $\vec{k}_i = \vec{k}_i^0 + \Delta\vec{k}_i$, with $|\Delta\vec{k}_s| \ll |\vec{k}_s^0|$ and $|\Delta\vec{k}_i| \ll |\vec{k}_i^0|$. The central wave vectors are dictated by the phase-matching conditions $\vec{k}_p = \vec{k}_s^0 + \vec{k}_i^0$, $\omega_p = \omega_s + \omega_i$, where ω_s and ω_i are the frequencies of the signal and idler photons. Introducing the azimuthal angles $\varphi_s^0 = 0$ and $\varphi_i^0 = \pi$, and the polar angles θ_s^0 and θ_i^0, the central wave vectors $\vec{k}_s^0$, $\vec{k}_i^0$ can be written as $\vec{k}_s^0 = (\omega_s n_s/c)[\sin\theta_s^0 \hat{x} + \cos\theta_s^0 \hat{z}]$ and $\vec{k}_i^0 = (\omega_i n_i/c)[-\sin\theta_i^0 \hat{x} + \cos\theta_i^0 \hat{z}]$, where n_s and n_i are the corresponding refractive indices. The width of the wave vectors bundles $\Delta\vec{k}_s$, $\Delta\vec{k}_i$, can be expressed in terms of the corresponding Fourier spatial frequencies p, q as $\Delta\vec{k}_s = p_s \cos\theta_s \hat{x} + q_s \hat{y} - p_s \sin\theta_s \hat{z}$, $\Delta\vec{k}_i = q_i \hat{y} + p_i \cos\theta_i \hat{x} + p_i \sin\theta_s \hat{z}$ [18]. For simplicity, here we make use of the thin crystal approximation, hence the phase-matching conditions are only applicable in the transverse directions [19]. Notwithstanding, we have verified that the general case of a thick crystal gives qualitatively analogous results. Finally, here we examine the case of degenerate type I interaction with $\theta_s^0 = \theta_i^0$ and $\omega_s = \omega_i$. The continuous wave approximation is justified by the use of narrow band interference filters in front of the detectors.

Under such conditions, the generated two-photon quantum state is found to be given by

$$|\Psi\rangle \sim d_\mathrm{eff} \int \mathrm{d}p_s \mathrm{d}q_s \mathrm{d}p_i \mathrm{d}q_i \hat{\Phi}\left[\cos\theta_s^0(p_s + p_i), q_s + q_i\right] \times a_s^\dagger(p_s, q_s) a_i^\dagger(p_i, q_i)|0,0\rangle, \tag{2}$$

where $a_{s,i}^\dagger$ are creation operators for the signal and idler modes, and $d_\mathrm{eff} = 1/2 \sum_{i,j,k} (\hat{e}_p)_i \chi_{ijk}^{(2)} (\hat{e}_s)_j^* (\hat{e}_i)_k^*$, where $\hat{e}_s$ and $\hat{e}_i$ stand for the polarization direction of the signal and idler modes, is the effective nonlinear coefficient. Note that in noncollinear geometries with large polar angles θ_s^0, θ_i^0 the polarization directions of the type I downconverted photons are no longer perpendicular to the polarization of the pump beam [20].

The entangled two-photon quantum state (2) is a coherent superposition of an infinite number of eigenstates of the corresponding OAM operators, which in each frame are represented by Laguerre–Gaussian (LG) mode functions. The normalized LG_p^l mode at its waist is given in cylindrical coordinates by

$$\mathrm{LG}_p^l(x,y,z=0) = \sqrt{\frac{2p!}{\pi(|l|+p)!}} \frac{1}{w_0} \left(\frac{\sqrt{2}\rho}{w_0}\right)^{|l|} L_p^{|l|}\left(\frac{2\rho^2}{w_0^2}\right) \times \exp(-\rho^2/w_0^2) \exp(\mathrm{i}l\varphi), \tag{3}$$

where $L_p^l(\rho)$ are the associated Laguerre polynomials, ρ is the radial cylindrical coordinate, w_0 is the mode width, p is the number of nonaxial radial nodes, and the index l, referred to as the winding number, describes the helical structure of the wave front. When the mode function of a single photon is a pure LG mode with winding number l, it corresponds to an eigenstate of the paraxial OAM operator with eigenvalue $l\hbar$ [21]. Expansion of the entangled two-photon state (2) into *noncollinear* OAM eigenstates centered on the axes dictated by the signal and idler central wave vectors, respectively, i.e., $|\Psi\rangle \sim \sum_{l_1,p_1}\sum_{l_2,p_2} C^{l_1,l_2}_{p_1,p_2}|l_1,p_1;l_2,p_2\rangle$, yield the amplitudes

$$C^{l_1,l_2}_{p_1,p_2} \sim d_{\mathrm{eff}} \int \mathrm{d}p_s\,\mathrm{d}q_s\,\mathrm{d}p_i\,\mathrm{d}q_i\,\hat{\Phi}\big(\cos\theta_s^0(p_s+p_i), q_s+q_i\big) \times \Big[\mathrm{LG}^{l_1}_{p_1}(p_s,q_s)\Big]^* \Big[\mathrm{LG}^{l_2}_{p_2}(p_i,q_i)\Big]^*, \qquad (4)$$

where $\mathrm{LG}^l_p(p,q)$ is the Fourier transform of $\mathrm{LG}^l_p(x,y)$. Eq. (4) can be written in the spatial domain as

$$C^{l_1,l_2}_{p_1,p_2} \sim d_{\mathrm{eff}} \int \mathrm{d}x\,\mathrm{d}y\,\Phi\left(\frac{x}{\cos\theta_s^0}, y\right) \Big[\mathrm{LG}^{l_1}_{p_1}(x,y)\Big]^* \times \Big[\mathrm{LG}^{l_2}_{p_2}(x,y)\Big]^*, \qquad (5)$$

where $\Phi(x,y)$ is the transverse spatial amplitude distribution. Eq. (5) is a central result of this paper. Notice that it only holds for $\theta_s^0 < 90°$, and that its derivation explicitly assumes that mode functions of the signal and idler photons are paraxial in their corresponding coordinate frame.

The transverse amplitude distribution of the pump beam $\Phi(x,y)$ can be expanded into spiral harmonics in the form $\Phi = 1/\sqrt{2\pi}\sum_{l=-\infty}^{\infty} a_l(\rho)$ $\exp(\mathrm{i}l\varphi)$. Therefore, (5) reveals that each amplitude $C^{l_1,l_2}_{p_1,p_2}$ depends only on the (l_1+l_2)th angular harmonic of the pump beam. Thus, in collinear phase-matching geometries (i.e., $\theta_s^0 = 0$), only the terms which verify $l_1 + l_2 = l_p$, where l_p is the winding number associated to the pump beam, contribute a nonvanishing amplitude probability $C^{l_1,l_2}_{p_1,p_2}$ [9]. However, the point is that because of the factor $\cos\theta_s^0$ appearing in Eq. (5), in noncollinear geometries the expansion $|\Psi\rangle \sim \sum_{l_1,p_1}\sum_{l_2,p_2} C^{l_1,l_2}_{p_1,p_2}$ $|l_1,p_1;l_2,p_2\rangle$ always contains contributions with $l_1 + l_2 \neq l_p$.

To elucidate the quantitative weight of such "anomalous" contributions, we considered a down-conversion process pumped by a Gaussian laser beam with a vortex nested on-axis (e.g., by a computer generated hologram), with the amplitude distribution

$$\Phi(x,y) \sim \big[x + \mathrm{i}\,\mathrm{sgn}(l_p)y\big]^{|l_p|} \exp\left\{-\frac{x^2+y^2}{w_p^2}\right\}, \qquad (6)$$

where l_p is the topological charge of the vortex, $\mathrm{sgn}(l_p)$ its helicity, and w_p the width of the host beam. Fig. 2 shows illustrative examples of the paraxial OAM eigenstate content of the generated entangled two-photon state for different values of the angle θ_s^0, in the case of a pump beam with $l_p = 4$. On physical grounds, as θ_s^0 increases, Eq. (5) can be viewed as the distribution existing in a collinear geometry but now by a vortex with internal structure, or noncanonical [22,23], nested in an elliptical beam. Thus, in nearly collinear configurations ($\theta_s^0 \simeq 0$), only the terms with $l_1 + l_2 = l_p$ exhibit relevant contributions, as shown in Fig. 2(a). In contrast, the contributions obtained when $\theta_s^0 = 45^0$ and $\theta_s^0 = 60^0$ are shown in Figs. 2(b) and (c), respectively. One finds that there are states featuring $l_1 + l_2 \neq l_p$ which make an even *higher contribution* to the two-photon state than that of states with $l_1 + l_2 = l_p$.

The total strength of the violation of the rule $l_1 + l_2 = l_p$ can be evaluated by projecting the signal photon into a state with well defined l_1, p_1 and then adding-up all the weights of the "anomalous" idler states. Here we report the outcome obtained for a signal photon projected into the state with mode function $F(x,y) = \exp\{-(x^2+y^2)/w_0^2\}$, which can be implemented experimentally by detecting the signal photon after propagation through a suitable spatial mode filter (e.g., a monomode optical fiber). The resulting mode function of the idler photon at the output of the crystal writes $G(x,y) \sim \Phi(x/\cos\theta_s^0, y)F(x,y)$. Then, the quantum state of the idler photon can be written as [8] $\langle s|\Psi\rangle = \sum_{n=-\infty}^{\infty} C_n|l=n\rangle$, where $|C_n|^2 = \int_0^\infty |a_n|^2 \rho\,\mathrm{d}\rho$, with $a_n = 1/(2\pi)^{1/2}\int_0^{2\pi} G(\rho,\varphi)\exp(-\mathrm{i}n\varphi)\,\mathrm{d}\varphi$, and the weights of the quantum superposition P_l are given by $P_l = |C_l|^2/\sum_{i=-\infty}^{\infty}|C_i|^2$. Therefore, the quantity $\delta = \sum_{l\neq l_p} P_l$, gives the probability to detect a coincidence between a signal photon with no paraxial angular momentum, and an idler photon with paraxial angular momentum $l_2\hbar$, but with $l_2 \neq l_p$. Fig. 3 shows the values of δ that we obtained for pump beams with $l_p = 4$ and $l_p = 10$, as a function of the noncollinear angle θ_s^0. The plot

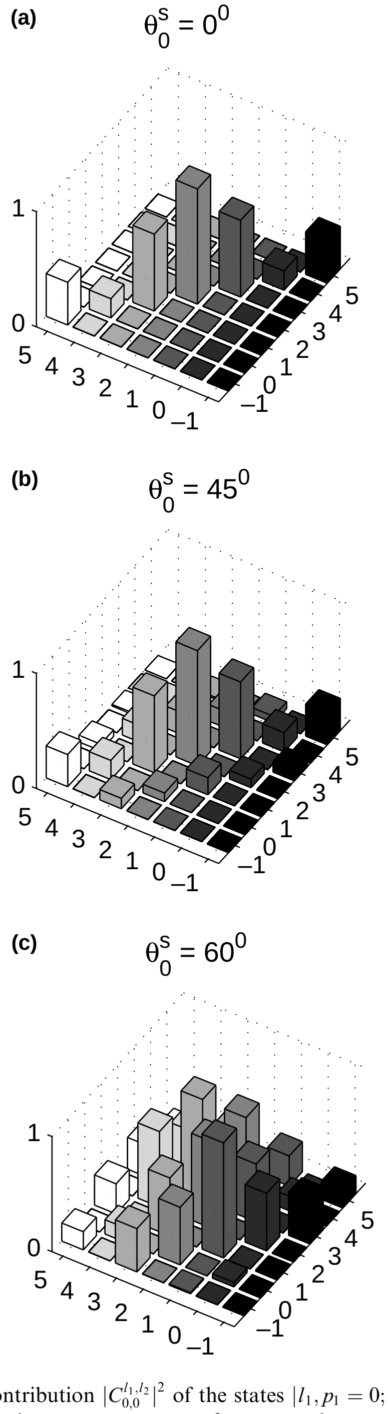

Fig. 2. Contribution $|C_{0,0}^{l_1,l_2}|^2$ of the states $|l_1, p_1 = 0; l_2, p_2 = 0\rangle$ to the two-photon quantum state for a pump beam with $l_p = 4$. (a) $\theta_s^0 = 0^0$, (b) $\theta_s^0 = 45^0$ and (c) $\theta_s^0 = 60^0$. All values are normalized to the maximum value of the distribution $C_{0,0}^{l_1,l_2}$ for each angle θ_s^0.

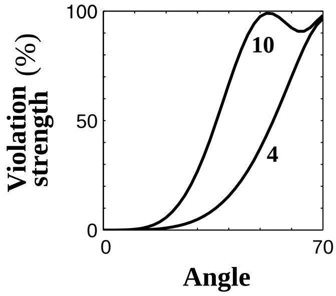

Fig. 3. Violation strength δ of the rule $l_1 + l_2 = l_p$ for a pump beam with $l_p = 4$ and 10, when the signal photon has been projected into a Gaussian mode function.

confirms that the strength of the violation increases nonmonotonically with the polar angle θ_s^0. Importantly, while $\delta \approx 0$ for all near paraxial phase-matching geometries, one finds that suitable polar angles do exist where *almost all* coincidence detections are predicted to correspond to photons that violate the rule $l_1 + l_2 = l_p$. In Fig. 4, we plot the weights of the idler quantum state for $\theta_s^0 = 60^0$ and $l_p = 10$, after the signal photon has been projected into a Gaussian mode function.

The experimental observation of this effect requires a phase-matched noncollinear geometry with large polar angles. At optical wavelengths in typical $\chi^{(2)}$ nonlinear crystals noncollinear phase-matching occurs with polar angles of a few degrees (e.g., 3° [24]), but phase-matching with $\theta \sim 18°$, where the effect should be already visible is possible, e.g., in β-barium borate and lithium iodate pumped with frequency-doubled Ti:Sa lasers [18,25]. However, quasi-phase-matching in periodically-poled materials appears to be the ideal setting to achieve

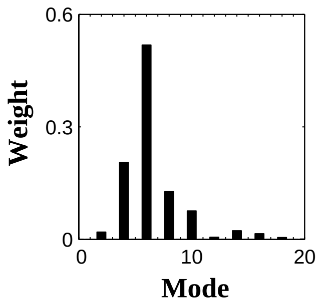

Fig. 4. Mode distribution of the quantum state of the idler for $\theta_s^0 = 60^0$. Pump beam and the signal photon as in Fig. 3.

phase-matching with arbitrary large noncollinear angles. For example, higher-order noncollinear quasi-phase-matched photon downconversion at $\theta \sim 60^\circ$ for $\lambda_p \sim 400$ nm can be achieved in periodically-poled lithium niobate with poling periods several microns long (thus well-inside the current technological state of the art [26]), with still a significant resulting $d_{eff} \sim 1$ pm/V, similar to that of critically-phase-matched β-barium borate.

To conclude, we stress that the effect predicted here has a purely geometrical origin, i.e., it is due to the noncollinear propagation directions of the photons emerging from the downconverting crystal, and is not related, e.g., to any exchange of angular momentum between light and matter. It is worth stressing that the paraxial operator yielding the anomalous values is a well-defined quantity for each of the photons, and that it corresponds to the quantity that is accessible in current experiments [7,11]. However, as the effect predicted here highlights, in noncollinear geometries it does not yield the angular momentum that must be conserved. Elucidation of the conserved angular momentum of the downconverted photons in noncollinear geometries requires a step forward in the development of the interaction picture of quantum electrodynamics, namely its application to *globally nonparaxial* [3], instead of *locally-paraxial*, photon mode functions and the corresponding *total* angular momentum operators.

Acknowledgements

This work was partially supported by the Generalitat de Catalunya, by the Spanish Government through grant BFM2002-2861 and by a Lise Meitner Fellowship.

References

[1] J.H. Poynting, Proc. R. Soc. London, Ser. A 82 (1909) 560; R.A. Beth, Phys. Rev. 50 (1936) 115.
[2] L. Allen, M.J. Padget, B. Babiker, in: E. Wolf (Ed.), Progress in Optics, vol. XXXIX, 1999, p. 291.
[3] C. Cohen-Tannoudji, J. Dupont-Roc, G. Grynberg, Photons and Atoms: Introduction to Quantum Electrodynamics, Wiley, New York, 1989.
[4] S.J. Van Enk, G. Nienhuis, J. Mod. Opt. 41 (1994) 963; Europhys. Lett. 25 (1994) 497.
[5] N.B. Simpson, K. Dholakia, L. Allen, M. Padgett, Opt. Lett. 22 (1997) 52.
[6] S.M. Barnett, J. Opt. B: Quantum Semiclass. Opt. 4 (2002) S7.
[7] A. Mair, A. Vaziri, G. Weihs, A. Zeilinger, Nature (London) 412 (2001) 313.
[8] G. Molina-Terriza, J.P. Torres, L. Torner, Phys. Rev. Lett. 88 (2002) 013601.
[9] S. Franke-Arnold, S.M. Barnett, M.J. Padgett, L. Allen, Phys. Rev. A 65 (2002) 033823;
M. Padgett, J. Courtial, L. Allen, S. Franke-Arnold, S. Barnett, J. Mod. Opt. 49 (2002) 777.
[10] A. Vaziri, G. Weihs, A. Zeilinger, G. Molina-Terriza, J.P. Torres, L. Torner, Opt. Photon News 13 (12) (2002) 54.
[11] A. Vaziri, G. Weihs, A. Zeilinger, Phys. Rev. Lett. 89 (2002) 240401.
[12] H.H. Arnaut, G.A. Barbosa, Phys. Rev. Lett. 85 (2000) 286; G.A. Barbosa, H.H. Arnaut, Phys. Rev. A 65 (2002) 053801.
[13] E.R. Eliel, S.M. Dutra, G. Nienhuis, J.P. Woerdman, Phys. Rev. Lett. 86 (2001) 5208;
J. Visser, E.R. Eliel, G. Nienhuis, Phys. Rev. A 66 (2002) 033814.
[14] D.P. Caetano et al., Phys. Rev. A 66 (2002) 041801(R).
[15] D.N. Klyshko, Sov. Phys. JEPT 28 (1969) 522.
[16] D.C. Burnham, D.L. Weinberg, Phys. Rev. Lett. 25 (1970) 84.
[17] C.K. Hong, L. Mandel, Phys. Rev. A 31 (1985) 2409.
[18] A. Joobeur, B.E.A. Saleh, T.S. Larchuk, M.C. Teich, Phys. Rev. A 53 (1996) 4360.
[19] B.E.A. Saleh, A.F. Abouraddy, A.V. Sergienko, M.C. Teich, Phys. Rev. A 62 (2000) 043816.
[20] A. Migdall, J. Opt. Soc. Am. B 14 (1997) 1093.
[21] L. Allen, M.W. Beijersbergen, R.J.C. Spreeuw, J.P. Woerdman, Phys. Rev. A 45 (1992) 8185.
[22] I. Freund, Opt. Commun. 159 (1999) 99;
Opt. Commun. 181 (2000) 19.
[23] G. Molina-Terriza, E.M. Wright, L. Torner, Opt. Lett. 26 (2001) 163.
[24] P.G. Kwiat, K. Mattle, H. Weinfurter, A. Zeilinger, A.V. Sergienko, Y. Shih, Phys. Rev. Lett. 75 (1995) 4337.
[25] V.G. Dmitriev, G.G. Gurzadyan, D.N. Nikogosyan, Handbook of Nonlinear Optical Crystals, Springer, Berlin, 1997.
[26] See, e.g., L. Gallmann, G. Steinmeyer, G. Imeshev, J.P. Meyn, M.M. Fejer, U. Keller, Appl. Phys. B 74 (2002) S237, and references therein.